Available online at www.sciencedirect.com
ScienceDirect
Journal of Colloid and Interface Science 317 (2008) 255–263
JOURNAL OF Colloid and Interface Science
www.elsevier.com/locate/jcis

Controlled chemical stabilization of self-assembled PS-P4VP nanostructures

Yeng Ming Lam [a,*], Lixin Song [a], Ya Chuin Moy [a], Lifei Xi [a], Chris Boothroyd [b]

[a] *School of Materials Science and Engineering, Nanyang Technological University, Nanyang Avenue, Singapore 639798, Republic of Singapore*
[b] *Institute of Materials Research and Engineering, 3 Research Link, Singapore 117602, Republic of Singapore*

Received 1 July 2007; accepted 11 September 2007

Available online 21 September 2007

Abstract

Supramolecular self-assemblies in selective solvents give rise to many patterning possibilities. The diblock copolymer polystyrene-*b*-poly(4-vinylpyridine) (PS-P4VP) is one such polymer that self-assembles into neat nanostructures in toluene. These nanostructures once formed are highly susceptible to solvent influence. Unfortunately, for use as nanotemplates and in the synthesis of nanoparticles, the susceptibility of the films to solvents can be a problem. In this study, we present a method to stabilize the structures through chemical means in solution. We used 1,4-dibromobutane in solution to chemically crosslink the pyridine residues of each of PS-P4VP to yield a series of stable spherical aggregates. In this way, the cross-linking ratio can be precisely controlled. The solution properties were studied using dynamic light scattering and small angle X-ray scattering and the morphology of the resulting micellar film was studied using transmission electron microscopy (TEM). The size of the micelles formed was found to be dependent on the amount of cross-linking and the shape of the PS-P4VP micelles remains stable when exposed to a selective solvent for PS.

Keywords: Self-assembly; Diblock; Copolymer; PS-P4VP

1. Introduction

Nanostructures formed by self-assembled copolymers have generated considerable interest because of their technological applications. Although these nanostructures are stable in time at a set of fixed conditions, their characteristics for a given system depend on the thermodynamic quality of the solvent and on temperature. For this reason, it is impossible to study these systems under different conditions, e.g., in a different solvent at a different temperature or at other concentrations. Prochaska and Baloch [1] and Tuzar et al. [2] circumvented this problem by stabilizing a particular micellar structure such as block copolymers with a polybutylene (PB) block by cross-linking of the micellar core, either by UV or fast electron irradiation.

Cross-linking is known to be important to the preservation of mesostructural ordering during swelling and incorporation of inorganic precursors [3]. Without cross-links, the block copolymer template rearranges extensively upon swelling, destroying the spatial patterning imposed by preprocessing. By introducing cross-linkers, however, it is possible to restrict re-arrangement of the block copolymer during swelling and thereby produce inorganic oxide films with mesostructures that closely mimic those of the template films.

Another possibility first examined by Wooley and coworkers [4,5] is to cross-link the corona of the micelles. These kinds of nanoparticles are designated as shell cross-linked micelles by these authors. They applied this concept to a large variety of block copolymers, mainly hydrophobic–hydrophilic copolymers with PAA or quaternized PVP as the water soluble block, which can be chemically cross-linked in their micellar forms. A similar approach has been described by Bütün et al. [6] for the synthesis of shell cross-linked micelles where core and shell are both hydrophilic.

An alternative to form core cross-linked nanostructures was reported by Ishizu [7]. He started with diblock copolymer films containing poly(4-vinylpyridine) with P4VP spherical or cylindrical microdomains. These domains were cross-linked with the vapor of 1,4-dibromobutane in solid state to obtain spherical and ribbon-like polymer nanostructures. The control in the

* Corresponding author.
E-mail address: ymlam@ntu.edu.sg (Y.M. Lam).

0021-9797/$ – see front matter
doi:10.1016/j.jcis.2007.09.044

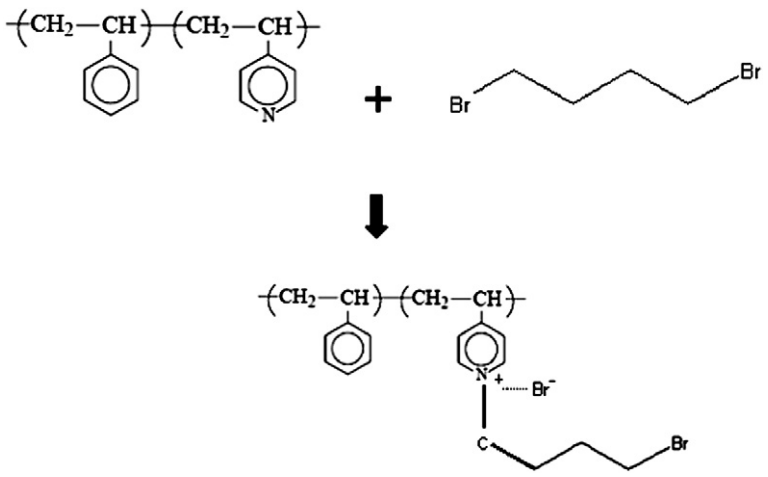

Scheme 1. Cross-linking of the P4VP by 1,4-dibromobutane.

degree of cross-linking achieved in this method may be more difficult and also, there may be cases where the surface micelles are cross-linked but the micelles further in the film might not be cross-linked.

In this work, we have chemically cross-linked self-assembled polystyrene-*b*-poly(4-vinylpyridine) (PS-P4VP) copolymers using 1,4-dibromobutane in solution. The effect of solvent treatment on the cross-linked block copolymer film has been investigated. The solution properties in toluene were studied using dynamic light scattering and small angle X-ray scattering (SAXS). Light scattering can provide information on the hydrodynamic dimensions of the micellar structures but it will not be able to provide any information on the internal structure such as core and shell dimensions of the micelles. As SAXS is based on the electron density differences in the structures, this technique will be able to provide information about the internal structures of the micelles. With a combination of these two techniques, we will be able to resolve the full structural information of the micelles. The morphology of the resulting micellar film was investigated using transmission electron microscopy (TEM). These studies confirmed that the morphology of the chemically stabilized spherical micelles are not affected by the selective solvents present. This has strong implications for its application as nanoreactors and nanotemplates where solvents may be present.

2. Experimental

2.1. Crosslinking of copolymer nanostructures

Polystyrene-block-poly(4-vinylpyridine) (PS-*b*-P4VP, $M_n^{PS} = 11{,}800$ g/mol, $M_n^{P4VP} = 15{,}000$ g/mol, $M_w/M_n = 1.04$) were obtained from Polymer Source, Inc. The cross-linking of the PS-P4VP diblock copolymer was carried out in toluene at 90 °C by using 1,4-dibromobutane (DBB). Refer to Scheme 1. The copolymer concentration was fixed at 5 mg/mL, while DBB was added at different amounts to reach the desired ratio (4VP:DBB = 10:0, 10:4, 10:6, 10:8, 10:10). The resulting solution containing cross-linked PS-P4VP was equilibrated for 1 day.

2.2. Fourier transform infrared spectroscopy

A Perkin Elmer System 2000 Fourier transform infrared spectrometer was used to characterize the polymer. First, a background spectrum was run with ground potassium bromide (KBr) die-pressed into flat circular pellet. Then drops of the copolymer sample were dropped onto the surface of KBr pellet. The spectrum of the mixed pellet was then collected against the spectrum of the background. A total of ten scans at a resolution of 4 cm^{-1} (in the mid IR region of 4000 to 400 cm^{-1}) were obtained to achieve a good signal-to-noise ratio. The key signal for the identification of the N–Br bond (465.2 cm^{-1}), which is formed between the cross-linking molecules 1,4-dibromobutane and the pyridine unit, was identified using a known compound—hexadecyltrimethylammonium bromide (HTAB). The HTAB has the molecular formula $(C_{16}H_{33})N(CH_3)_3Br$. Another key signal is the non-conjugated C–N stretching vibrations at 2260 cm^{-1}.

2.3. Laser light scattering

A Brookhaven BIS200SM laser scattering system equipped with a 522-channel Brookhaven BI9000 digital multiple τ correlator was used to perform both the static and the dynamic light scattering experiments. The light source is a power adjustable vertically polarized 35 mW argon ion laser with a wavelength of 632.8 nm. REPES [8] inverse Laplace transform of supplied with the GENDIST software package, was used to analyze the time correlation function (TCF), and the probability of rejection was set to 0.5.

Dynamic light laser scattering measures the temporal fluctuations of the scattered light produced by Brownian movement of the scattering particles [9]. This temporal variation of scattered radiation yields the Doppler shift, and the broadening of the central Rayleigh line could be used to determine the dynamic properties of the system. The intensity of the scattered light can be analyzed by proton correlation spectroscopy (PCS) [10–12].

The intensity–intensity autocorrelation function is expressed as

$$g_2(t) = \frac{\langle I(t)I(t+\tau)\rangle}{\langle I(t)^2\rangle},$$

where $I(t)$ is an average value of the products of the scattered intensity at an arbitrary time, t, and $I(t+\tau)$ is the intensity registered at delay time τ. The normalized field autocorrelation function is described by the expression

$$g_1(t) = \int w(\Gamma)\exp(-\Gamma t)\,d\Gamma,$$

where $w(\Gamma)$ is a continuous distribution function of decay rate Γ, which is the inverse of the decay time τ. If the inverse Laplace transform (ILT) is used to analyze the autocorrelation function, the decay time distribution function $w(\Gamma)$ can be obtained. For the translational diffusion mode, when the measurement angle θ is close to 0, the translational diffusion coefficient D is related to the decay rate by the expression

$$D = \frac{\Gamma}{q^2}.$$

The decay rates and the square of the scattering vector q exhibit a linear relationship, indicating that the decay is due to the translational diffusion of the aggregates in solution. For the translational diffusion mode of large aggregates, the hydrodynamic radius can be determined form the Stokes–Einstein equation

$$R_\mathrm{h} = \frac{kT}{6\pi\eta_0 D_0},$$

where η_0 is the viscosity of the solvent, T the absolute temperature, D_0 the translational diffusion coefficient at infinite dilution, and k the Boltzmann constant. If the diffusion coefficient in a dilute solution D is used instead of D_0, the apparent hydrodynamic radius is obtained.

2.4. Small angle X-ray scattering

A SAXSess camera (Anton-Paar, Graz, Austria) with an X-ray generator (PANalytical, PW3830, standalone laboratory X-ray source) operating at 40 kV and 50 mV with a sealed-tube Cu anode was used to perform the small angle X-ray scattering experiments. A Göbel mirror was used to convert the divergent polychromatic X-ray beam into a collimated line-shaped beam of Cu$K\alpha$ radiation ($\lambda = 0.154$ nm). The two-dimensional scattering pattern was collected on an imaging plate and then integrated into a one-dimensional scattering function $I(q)$ using SAXSQuant software from Anton-Paar. The solution was held in a quartz capillary holder and the scan was carried out at 25 °C.

The small angle data was evaluated using an indirect Fourier transform [13–15] followed by deconvolution [16–18]. The pair distance distribution function (PDDF), $p(r)$, can be used to determine the overall shape and size of the scattering particles. It is related to the intensity by the equation

$$I(q) = 4\pi\int_0^\infty p(r)\frac{\sin(qr)}{qr}\,dr,$$

where q is the magnitude of the scattering vector, q, defined as

$$q = \frac{4\pi}{\lambda}\sin\left(\frac{\theta}{2}\right),$$

where λ is the wavelength of the incident radiation (0.154 nm) and θ is the angle between the incident and the scattered beam.

In the case of a particle with a particular shape, the electron density contrast, $\Delta\rho(r)$, is related to the PDDF by

$$p(r) = r^2\Delta\tilde{\rho}^2(r),$$

where $\Delta\tilde{\rho}^2(r)$ is the convolution square of $\Delta\rho(r)$ averaged for all directions in space [16,17]. This averaging for the case of a spherical particle will not result in the loss of information.

2.5. Transmission electron microscopy

The samples were prepared by one of two methods: solution dropped onto a holey carbon film and dried in vacuum for 24 h; or solution spin coated onto a piece of freshly cleaved mica, dried and the film floated in water and picked up using a copper grid. They were then stained with iodine vapor at 80 °C for an hour in a capped container. Transmission electron microscopy (TEM) was performed using a JEOL 2010 200 kV LaB_6 microscope operating at a magnification of 30,000×.

3. Results and discussion

3.1. Chemical analysis

Normalized FTIR spectra from cross-linked PS-P4VP were obtained for various cross-linking ratios (4VP:DBB = 10:10, 10:8, 10:6, 10:4, 10:0) as shown in Fig. 1a. The appearance of the quaternized pyridine absorption at 840 and 1640 cm^{-1} was observed for the cross-linked samples [7a]. This provide an evidence of the presence of the cross-links.

A peak at 462.67 cm^{-1} is evident in the four samples with cross-linker, but not in the spectrum with no dibromobutane added. This suggests the peak at 462.67 cm^{-1} is associated with 4VP-dibromobutane cross-linking. This is confirmed by looking that the IR spectrum for HTAB in Fig. 1b. The non-conjugated C–N stretching vibrations at 2260 cm^{-1} which becomes more significant as the cross-linking ratio increases. The percentage of the cross-linking can be calculated by integrating the area of the peak associating with N–Br bond (462.67 cm^{-1}). Assuming that 100% cross-linking occurred at 10:10, it is found that the cross-linking percentage are 48%, 57% and 96% for 10:4, 10:6 and 10:8, respectively. With the increase in the amount of DBB, there is a corresponding increase in the percentage of cross-links.

3.2. Solution behavior

3.2.1. Dynamic light scattering (DLS)

Dynamic light scattering measurements were carried out to measure the micellar dimensions for different cross-linking ratios. Using Stokes–Einstein relationship, the hydrodynamic radii were calculated. For Stokes–Einstein relationship to be

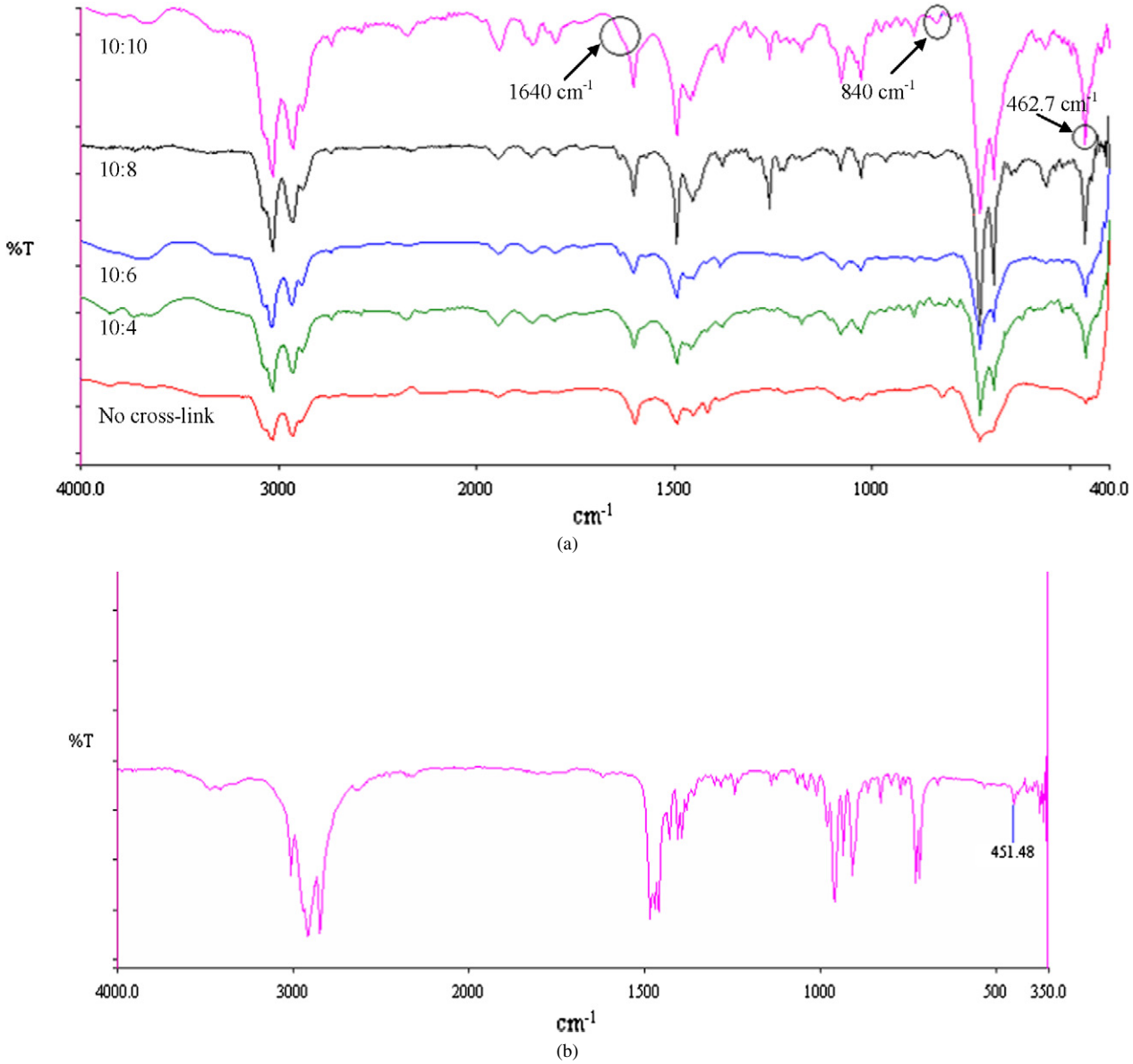

Fig. 1. (a) Normalized FTIR spectra of PS-P4VP samples with varying cross-linker ratios (4VP-DBB = 10:0, 10:4, 10:6, 10:8, 10:10). (b) FTIR spectrum of hexadecyltrimethylammonium bromide (HTAB).

applied, the micelles are assumed to be spherical, monodisperse, dilute and non-interacting. In the TEM micrographs of the thin film samples, it can be observed that the micelles are indeed spherical and monodispersed. As the concentration of the samples are kept very low (5 mg/mL), the criteria for dilute and non-interacting system is fulfilled. The apparent hydrodynamic radii (R_h) of the cross-linked PS-P4VP) were obtained for cross-linking ratios of 4VP:DBB = 10:10, 10:8, 10:6, 10:4, 10:0 as shown in Table 1.

Table 1
Micellar dimensions from dynamic light scattering

Cross-linking (4VP:DBB)	Hydrodynamic radii (nm)	Polydispersity
No cross-linking	22.9	0.03
10:4	23.2	0.005
10:6	23.7	0.019
10:8	24.2	0.016
10:10	26.8	0.088

The decay time distribution functions of typical cross-linked PS-P4VP in toluene at 4VP:DBB at 298 K are shown in Fig. 2a. $A(\tau)$ is the distribution of relaxation times in GEX (general exponential) model [19]. From Fig. 2a, it can be seen that there is one main relaxation peak in the time distribution plot. The peak shifts to the left when the measurement angle is increased. The relaxation process caused by the translational diffusion movement of the molecules exhibits the following relationship between relaxation time and the scattering vector [9]:

$$\tau \propto 1/\sin^2(\theta/2).$$

This relation can be used to interpret the peak shift as a function of measuring angle. Since $\tau \propto 1/\sin^2(\theta/2)$ for $0 < \theta < 180°$, $1/\sin^2(\theta/2)$ would decrease with increasing angle θ.

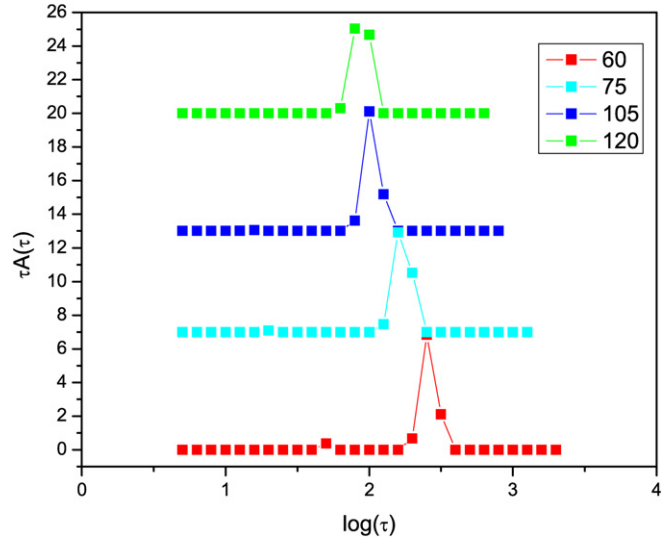

(a)

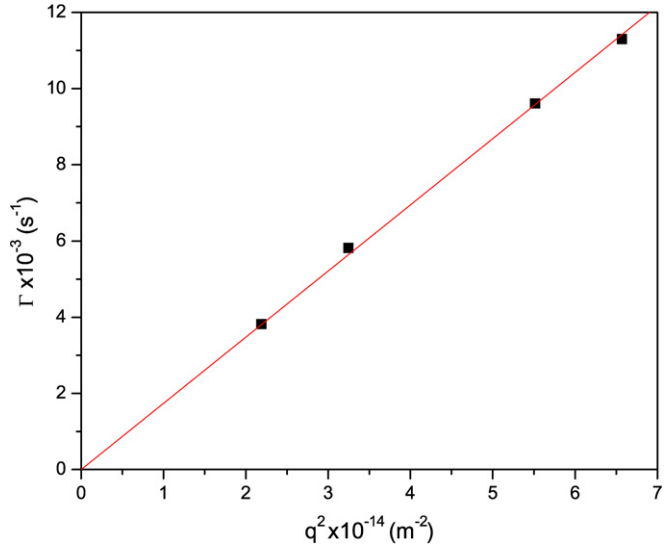

(b)

Fig. 2. (a) Decay time distribution function at different angles and (b) relationship between relaxation rates Γ and q^2 for PS-P4VP with 4VP:DBB = 10:6 at 298 K.

The q^2 dependence of Γ (Fig. 2b) exhibits a linear relationship and goes through the origin, which confirms that the peak is due to the translational diffusion of the aggregates in solution. On the basis of the diffusion coefficients, the apparent hydrodynamic radii of slow modes were also determined from the Stokes–Einstein equation. The size distribution consists of a large peak with an average R_h of about 47.4 nm. The decay mode in the relaxation time distribution is attributed to interchain associative aggregates (47.4 nm) and other aggregates [20,21]. Looking at the results from the light scattering data, it can be concluded that the dimension of the aggregates with and without cross-linking are relatively consistent except for the aggregate with 4VP:DBB = 10:10. The reason for the increase in dimension for large cross-linking ratio may be due to either the expansion of the core and hence the size of the aggregates or the presence of a large amount of the 1,4-dibromobutane in the solvent which helps to improve the solvent quality for PS. In order to determine which is the reason, we use small angle X-ray scattering to determine the core-shell dimensions of the aggregates.

3.2.2. *Small angle x-ray scattering*

The cross-linked PS-P4VP at different 4VP:DBB were characterized by SAXS. As slit collimation of the primary beam was used in the experimental setup, desmearing of the scattering curve was required and this was done using the indirect Fourier transformation (IFT) algorithm [13–15] using the general inverse Fourier transform (GIFT) routine. The experimentally measured SAXS curves were used to calculate the pair distance distribution function (PDDF) using IFT and by deconvolution of the PDDF, the radial contrast profile $\Delta\rho(r)$ was obtained. Fig. 3 shows the PDDF and the corresponding fits from the deconvolution of the scattering. Since the PDDFs of all the six systems are relatively symmetrical, one can assume the shape of the micelles are spherical for all six solutions. The shapes for the PDDF for the micelles with and without cross-linking are basically the same. Looking at the PDDF, it is obvious that the sizes of the non-cross-linked micelles are smaller (26 nm). When the 4VP:DBB ratio increased to 10:4, the size of the micelles increased to 28 nm. At ratios above 10:6, the size of the micelles remained at 32 nm.

In Fig. 4, the radial contrast profiles from the deconvolution using spherical symmetry are shown and step functions were used to build up the contrast profile. From the contrast profile, it can be observed that the contrast from the lyophobic and lyophilic blocks of the chains are very similar in cases where there is no cross-linking. This is expected as the only difference between the poly(4-vinylpyridine) and the polystyrene group is that one of the C atoms in styrene is replaced by N in 4-vinylpyridine. In the case when there is no cross-linking, it is difficult to differentiate the core from the shell. When there is cross-linking, the shell electron density remains the same but the electron density of the core increases. Hence, the electron density contrast between the shell and the core increased and the shell of the micelles can be determined. The dimensions of the micelles are shown in Table 2. As the cross-linker content increase from 4VP:DBB = 10:4 to 10:6, the diameter of the core increased from 16 to 20 nm and this result in a corresponding increase in the size of the micelles/aggregates. Above ratio of 4VP:DBB = 10:6, the dimension of the cores and the aggregates remains constant. The increase in the dimension observed in DLS for ratio 4VP:DBB is most probably due to an improve good solvent quality provided by the presence of the cross-linker rather than an increase in core dimensions. Also, the diameter of the micelles measured using DLS is somewhat larger than that determined by SAXS. The reason for the difference between the dimensions observed in DLS and SAXS is because PS in the PS-P4VP diblock copolymer has a very strong interaction with toluene. Hence in DLS, the value of the aggregate measure will include the associated toluene molecules. In DLS, any changes to the solvent quality will result in substantial changes to the dimension measured. Therefore, SAXS gives a more accurate measure of the aggregates dimen-

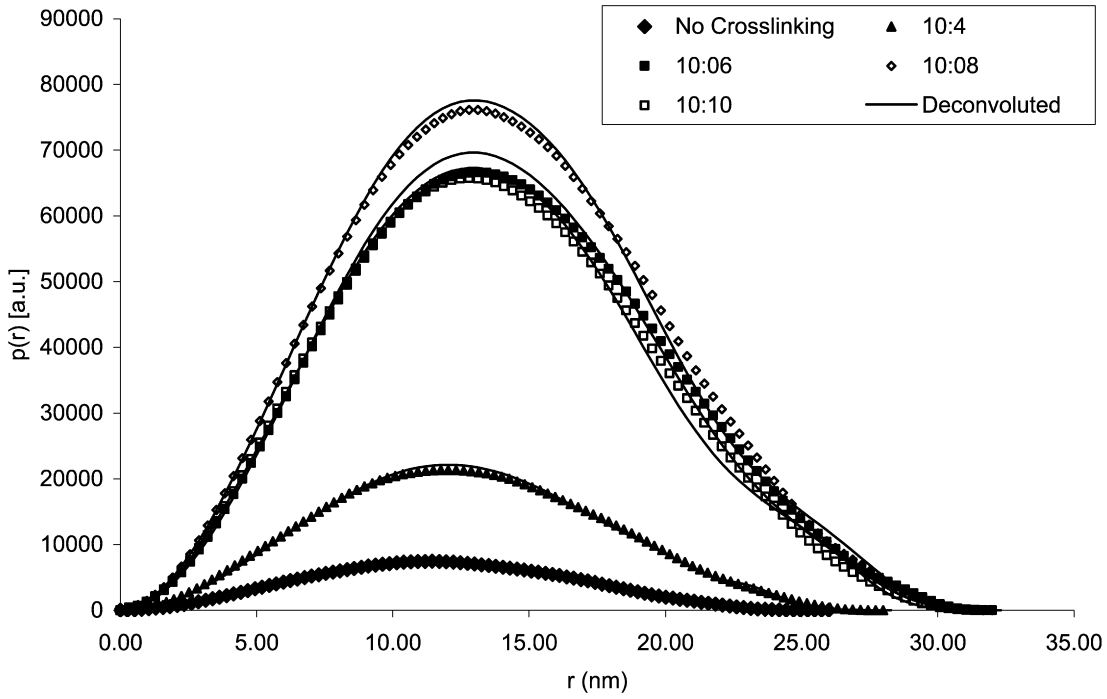

Fig. 3. Pair distance distribution function for solutions as the cross-linking ratios (4VP:DBB) is changed.

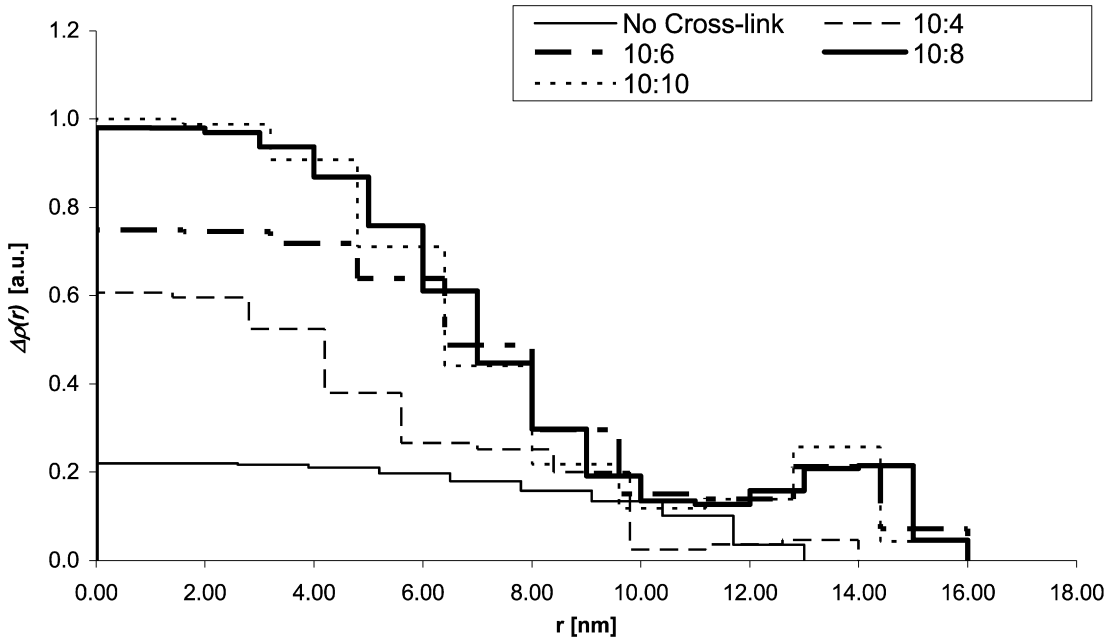

Fig. 4. Radial contrast profile $\Delta\rho(r)$ of the spectra of the solutions as a function of the cross-linking ratio (4VP:DBB).

sions. To confirm the dimensions of the aggregates and also to look at the stability of these aggregates, we will next look at their thin film behavior and the effect of exposing the self-assembled films to the selective solvent vapor treatment.

3.2.3. Thin film behavior

To determine the thin film morphologies of the various cross-linking ratios, the solution are either drop cast onto holey carbon grids or onto a mica substrate and then picked up with a copper grid. Without cross linking, the two preparation meth-

Table 2
Micellar dimensions from deconvolution using a single step model

Cross-linking (4VP:DBB)	Radii (nm)	Core radii (nm)	Shell thickness (nm)
No cross-linking	13	–	–
10:4	14	9	5
10:6	16	11	5
10:8	16	11	5
10:10	16	11	5

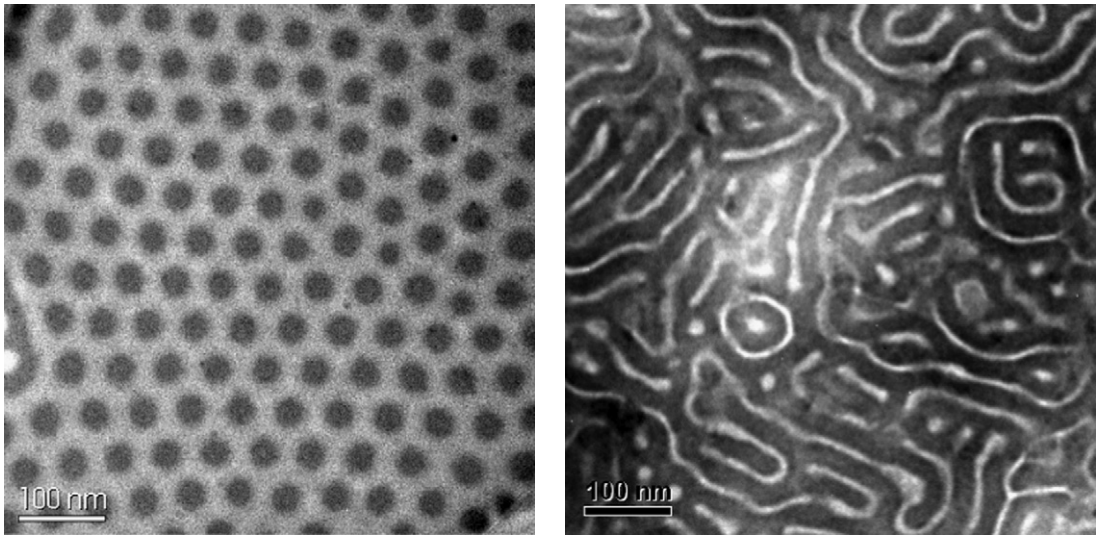

(a) (b)

Fig. 5. TEM image of the copolymer film of PS-P4VP without cross-linking prepared by (a) drop casting directly onto a holey carbon grid and (b) casting on mica followed by floating in water and picked up using a copper grid.

ods yield very difference morphologies. From Fig. 5a, using a direct casting method, with no contact with polar solvents such as water, the aggregates remain intact and the thin film morphology is consistently spherical throughout the film. As toluene is a selective solvent (a good solvent for PS but a poor solvent for P4VP), the P4VP block collapses to minimize the unfavorable interaction with toluene, while the PS block surrounding the P4VP block further preventing the interaction between the P4VP and toluene. Therefore in this case, the P4VP blocks and PS blocks form the micellar cores and shells respectively and these micelles are arranged into a regular hexagonal pattern. Looking at Fig. 5, the dark regions are P4VP blocks stained with iodine and the gray region is the PS blocks. If during the thin film preparation the film is exposed to a non-polar solvent that will affect the PS part of the chain or a polar solvent such as water (Fig. 5b), the polar solvent will result in an expansion of the cores due to preferential segregation of the solvent to the cores resulting in a ribbon like morphology. This is similar to what we have reported earlier [22,23].

At a 4VP:DBB ratio of 10:4, the cross-linking micelles diameter is seen to be about 33 nm which is very close to that determined using SAXS. The diameters of the micelles for cross-linked samples with 4VP:DBB ratios of 10:6, 10:8 and 10:10, as shown in Figs. 6b–6d, are about 31 nm which are comparable to the dimensions determined by SAXS. In addition, the core is found to have a diameter of about 23 nm which is again comparable to that determined from SAXS.

From the thin film studies, it is also observed that the cross-linked micelles are monodispersed even at high concentration

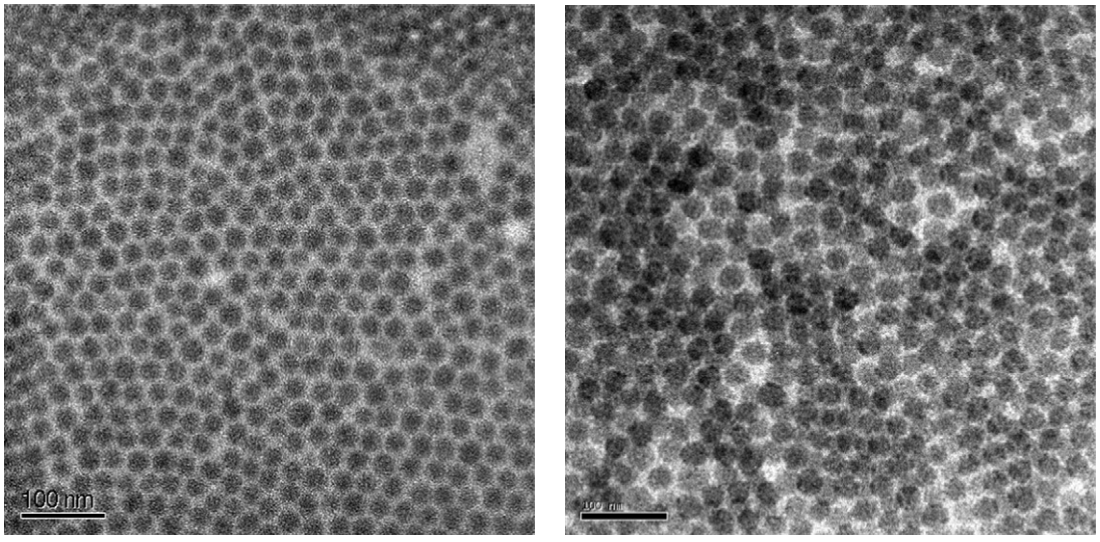

(a) (b)

Fig. 6. TEM images of cross-linked copolymer film for P4VP: DBB ratios of (a) 10:4, (b) 10:6, (c) 10:8, and (d) 10:10.

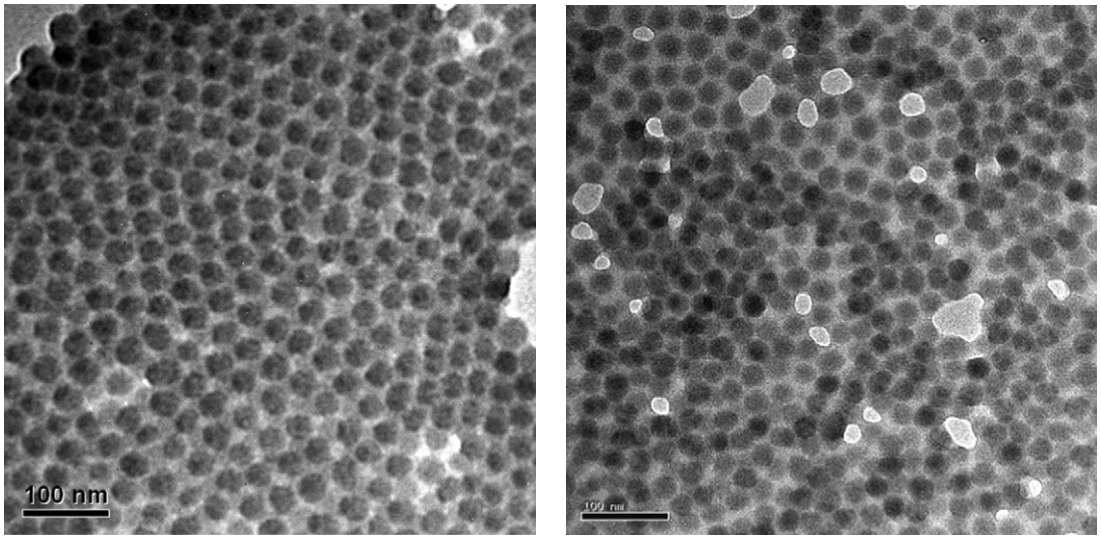

(c) (d)

Fig. 6. (*continued*)

of cross-links. This indicates that this method provides a viable route to cross-link PS-P4VP.

3.2.4. Solvent treatment

In order to show that the cross-linked micelles are stable when exposed to a selective solvent for P4VP such as toluene, the thin films were exposed to toluene vapor at elevated temperature for an extended time. The results are shown in Fig. 7. As we can see, the film without cross-linking lost its organized structure after exposure to solvents in very short time. The cross-linked films show no changes when exposed to toluene for an extended time. The stability of the film can be maintained even at a cross-linking percentage of about 50% which can be achieved at 4VP:DBB ratio of 10:4 and 10:6. The subsequent fusion between the cores due to the solvent can be prohibited when the cores are cross-linked. This is important when the pyridine units are required for coordination with precursors.

4. Conclusions

Polystyrene-*b*-poly(4-vinylpyridine) (PS-P4VP) copolymers can be cross-linked controllably through the use of dibromobutane as the cross-linker in solution. The new chemical bonds formed from the cross-linking can be studied using FTIR. The diameter of the cross-linked cores increase slightly compared to the uncross-linked cores. The cross-linked ratio necessary to stabilize the structures can be as low as 4:10 DBB to 4VP ratio leaving other pyridine units free for other chemical reactions. Cross-linking the copolymer in solution will give rise to a monodispersed morphology. This is true even up to very high

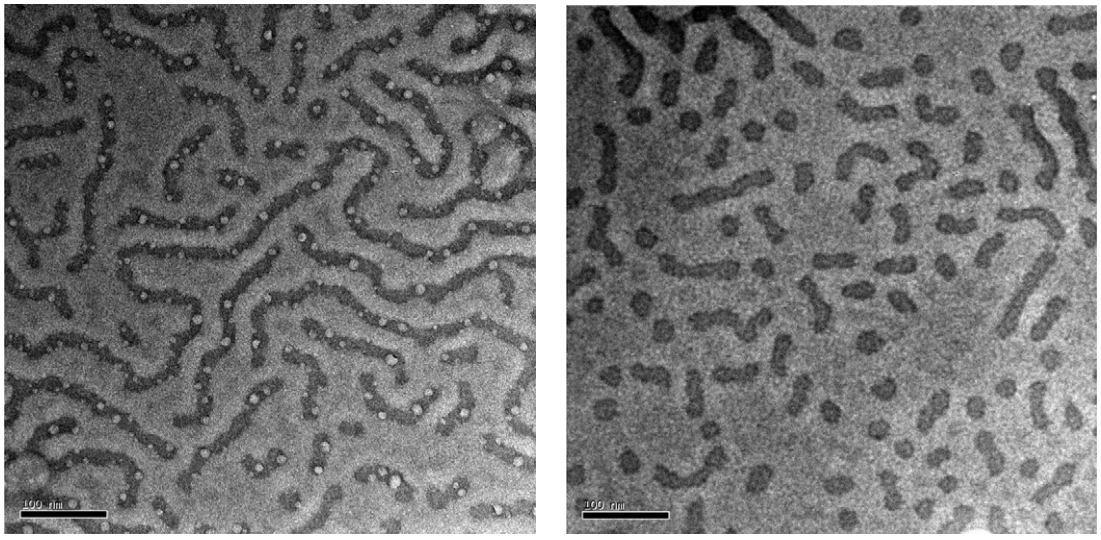

(a) (b)

Fig. 7. TEM image of cross-linked copolymer film as a function of P4VP:DBB ratio and solvent (toluene) treatment times: (a) no cross-linking, 1 h; (b) no cross-linking, 3 h; (c) 10:6, 1 h; (d) 10:6, 3 h; (e) 10:10, 1 h; (f) 10:10, 3 h.

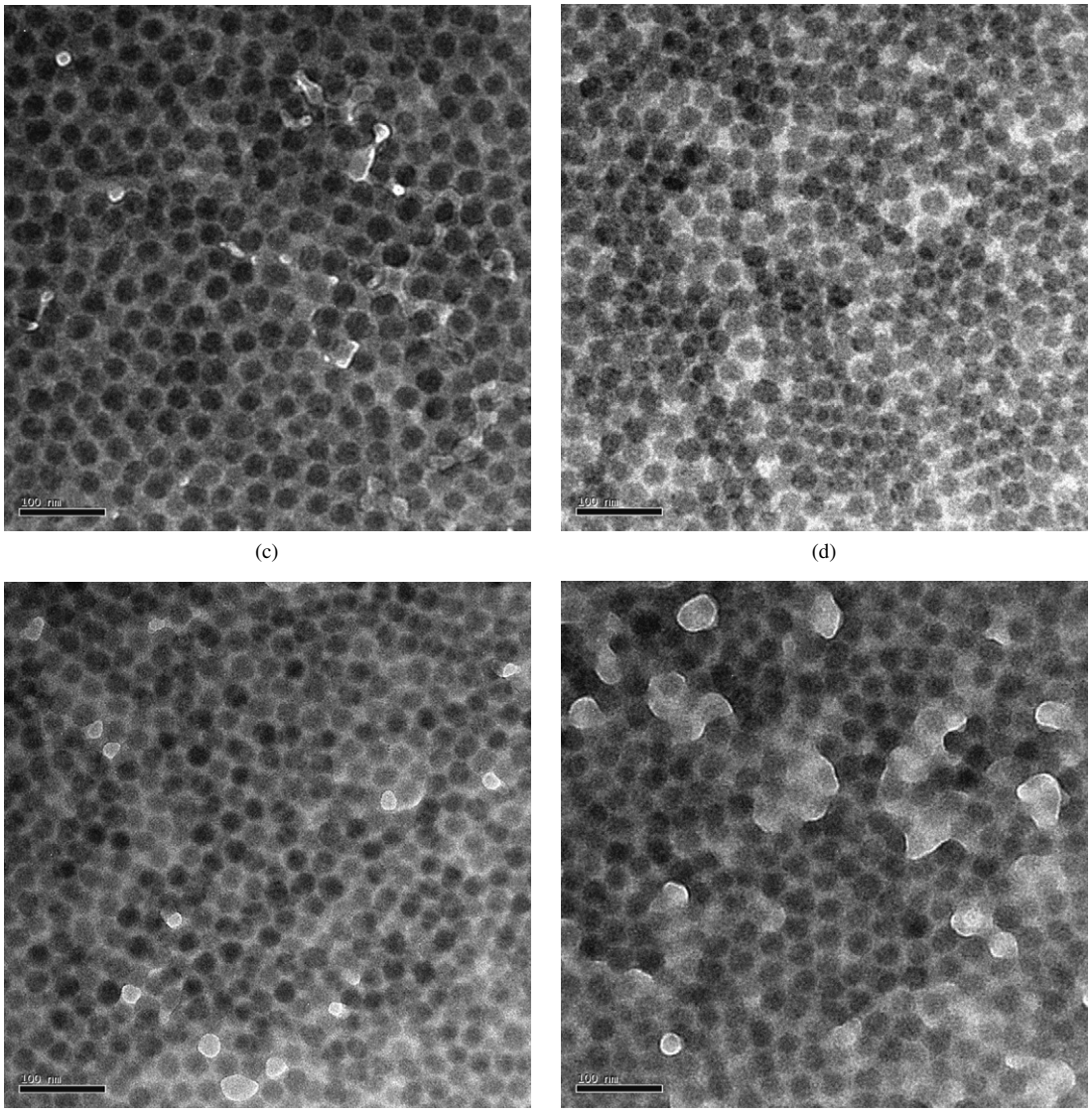

(c) (d)

(e) (f)

Fig. 7. (*continued*)

concentration of cross-links. This provides a better control of the cross-linking process as compared to the cross-linking using DBB vapor [7a]. This system is believed to have potential as a vehicle for highly stable nanoreactor applications.

References

[1] K. Prochaska, M.K. Baloch, Makromol. Chem. 180 (1979) 2521–2523.
[2] Z. Tuzar, B. Bednar, C. Konak, M. Kubin, S. Svobodova, K. Prochaska, Makromol. Chem. 183 (1982) 399–408.
[3] R.C. Hayward, B.F. Chmelka, E.J. Kramer, Macromolecules 38 (18) (2005) 7768–7783.
[4] K.B. Thurmond, T. Kowalewski, K.L. Wooley, ACS Polym. Prepr. (Div. Polym. Chem.) 38 (1) (1997) 62–63.
[5] Q. Ma, E.E. Remsen, T. Kowalewski, K.L. Wooley, ACS Polym. Prepr. (Div. Polym. Chem.) 41 (2) (2000) 1571–1572.
[6] V. Bütün, N.C. Billingham, S.P. Armes, J. Am. Chem. Soc. 121 (1999) 4288–4289.
[7] (a) K. Ishizu, Polymer 30 (1989) 793–798;
(b) K. Ishizu, T. Ikemoto, A. Ichimura, Polymer 40 (1999) 3147–3151.
[8] J. Jakes, Czech. J. Phys. B 38 (1988) 1305.
[9] S. Dai, K.C. Tam, R.D. Jenkins, Macromolecules 33 (2000) 404.
[10] W. Brown, Dynamic Light Scattering—The Method and Some Applications, Clarendon Press, Boston, 1993.
[11] B. Chu, Laser Light Scattering—Basic Principles and Principle, second ed., Academic Press, Boston, 1991.
[12] W. Brown, Light Scattering—Principles and Development, University Press, Oxford, 1996.
[13] O. Glatter, J. Appl. Crystallogr. 10 (1977) 415–421.
[14] O. Glatter, J. Appl. Crystallogr. 13 (1980) 577–584.
[15] O. Glatter, O. Kratky (Eds.), Small-Angle X-Ray Scattering, Academic Press, London, 1982.
[16] O. Glatter, J. Appl. Crystallogr. 14 (1981) 101.
[17] O. Glatter, B. Hainisch, J. Appl. Crystallogr. 17 (1984) 435–441.
[18] R. Mittelbach, O. Glatter, B. Hainisch, J. Appl. Crystallogr. 31 (1998) 600–608.
[19] http://www.fki.uu.se/robert.johnsen/gendist.htm.
[20] X.H. Wang, S.H. Goh, Z.H. Lu, S.Y. Lee, C. Wu, Macromolecules 32 (1999) 2786.
[21] C.Z. Li, W.C. Zhang, P. Zhou, F.S. Du, Z.C. Li, M.F. Li, Acta Polym. Sin. 4 (2001) 557.
[22] L. Song, Y.M. Lam, Nanotechnology 18 (2007) 075304.
[23] L. Song, Y.M. Lam, J. Nanosci. Nanotechnol. 6 (2006) 3904–3909.